



ELSEVIER

Contents lists available at ScienceDirect

## Physics Letters B

journal homepage: [www.elsevier.com/locate/physletb](http://www.elsevier.com/locate/physletb)

Letter



## Low-uncertainty measurement of the $^{239}\text{Pu}(n,f)$ cross section at n\_TOF in a very broad energy range from 0.02 eV up to 10 MeV

A. Sánchez-Caballero<sup>a,\*</sup>, D. Cano-Ott<sup>a</sup>, E. Mendoza<sup>a</sup>, V. Alcayne<sup>a</sup>,  
 J. Andrzejewski<sup>b</sup>, R. Capote<sup>c</sup>, T. Cardinaels<sup>d</sup>, P. Dries<sup>d</sup>, J. García Pérez<sup>a</sup>,  
 A. Gawlik-Ramiega<sup>b</sup>, E. González-Romero<sup>a</sup>, J. Heyse<sup>e</sup>, G. Leinders<sup>d</sup>, T. Martínez<sup>a</sup>,  
 G. Noguere<sup>f</sup>, C. Paradela<sup>e</sup>, A. Pérez De Rada Fiol<sup>a</sup>, J. Perkowski<sup>b</sup>, A. Plompen<sup>e</sup>,  
 P. Schillebeeckx<sup>e</sup>, G. Sibbens<sup>e</sup>, K. Van Hecke<sup>d</sup>, D. Vanleeuw<sup>e</sup>, K. Verguts<sup>d</sup>, M. Verwerft<sup>d</sup>,  
 D. Villamarin<sup>a</sup>, R. Wynants<sup>e</sup>, O. Aberle<sup>g</sup>, S. Altieri<sup>h,i</sup>, S. Amaducci<sup>j</sup>, V. Babiano-Suarez<sup>k</sup>,  
 M. Bacak<sup>g</sup>, J. Balibrea-Correa<sup>k</sup>, C. Beltrami<sup>h</sup>, S. Bennett<sup>l</sup>, A. P. Bernardes<sup>g</sup>, E. Berthoumieux<sup>m</sup>,  
 R. Beyer<sup>n</sup>, M. Boromiza<sup>o</sup>, D. Bosnar<sup>p</sup>, M. Caamaño<sup>q</sup>, F. Calviño<sup>r</sup>, M. Calviani<sup>g</sup>, A. Casanovas<sup>r</sup>,  
 D. M. Castelluccio<sup>s,t</sup>, F. Cerutti<sup>g</sup>, G. Cescutti<sup>u,v</sup>, S. Chasapoglou<sup>w</sup>, E. Chiaveri<sup>g,l</sup>,  
 P. Colombetti<sup>x,y</sup>, N. Colonna<sup>z</sup>, P. Console Camprini<sup>t,s</sup>, G. Cortés<sup>r</sup>, M. A. Cortés-Giraldo<sup>aa</sup>,  
 L. Cosentino<sup>j</sup>, S. Cristallo<sup>ab,ac</sup>, S. F. Dellmann<sup>ad</sup>, M. Diakaki<sup>w</sup>, M. Di Castro<sup>g</sup>, M. Dietz<sup>ae</sup>,  
 S. Di Maria<sup>af</sup>, C. Domingo-Pardo<sup>k</sup>, R. Dressler<sup>ag</sup>, E. Dupont<sup>m</sup>, I. Durán<sup>q</sup>, Z. Eleme<sup>ah</sup>,  
 S. Fargier<sup>g</sup>, B. Fernández<sup>aa</sup>, B. Fernández-Domínguez<sup>q</sup>, P. Finocchiaro<sup>j</sup>, S. Fiore<sup>s</sup>, V. Furman<sup>ai</sup>,  
 F. García-Infantes<sup>aj,g</sup>, G. Gervino<sup>x,y</sup>, S. Gilardoni<sup>g</sup>, C. Guerrero<sup>aa</sup>, F. Gunsing<sup>m</sup>, C. Gustavino<sup>ak</sup>,  
 W. Hillman<sup>l</sup>, D. G. Jenkins<sup>al</sup>, E. Jericha<sup>am</sup>, A. Junghans<sup>n</sup>, Y. Kadi<sup>g</sup>, K. Kaperoni<sup>w</sup>, G. Kaur<sup>m</sup>,  
 A. Kimura<sup>an</sup>, I. Knapová<sup>ao</sup>, M. Kokkoris<sup>w</sup>, Y. Kopatch<sup>ai</sup>, M. Krtička<sup>ao</sup>, N. Kyritsis<sup>w</sup>,  
 I. Ladarescu<sup>k</sup>, C. Lederer-Woods<sup>ap</sup>, J. Lerendegui-Marco<sup>k</sup>, G. Lerner<sup>g</sup>, A. Manna<sup>t,aq</sup>, A. Masi<sup>g</sup>,  
 C. Massimi<sup>t,aq</sup>, P. Mastinu<sup>ar</sup>, M. Mastromarco<sup>z,as</sup>, E. A. Maugeri<sup>ag</sup>, A. Mazzone<sup>z,at</sup>,  
 A. Mengoni<sup>s,t</sup>, V. Michalopoulou<sup>w</sup>, P. M. Milazzo<sup>u</sup>, R. Mucciola<sup>ab,au</sup>, F. Murtas<sup>av</sup>,  
 E. Musacchio González<sup>ar</sup>, A. Musumarra<sup>aw,ax</sup>, A. Negret<sup>o</sup>, N. Patronis<sup>ah,g</sup>, J. A. Pavón<sup>aa,g</sup>,  
 M. G. Pellegriti<sup>aw</sup>, P. Pérez-Maroto<sup>aa</sup>, C. Petrone<sup>o</sup>, E. Pirovano<sup>ae</sup>, J. Plaza Del Olmo<sup>a</sup>,  
 S. Pomp<sup>ay</sup>, I. Porras<sup>aj</sup>, J. Praena<sup>aj</sup>, J. M. Quesada<sup>aa</sup>, R. Reifarh<sup>ad</sup>, D. Rochman<sup>ag</sup>,  
 Y. Romanets<sup>af</sup>, C. Rubbia<sup>g</sup>, M. Sabaté-Gilarte<sup>g</sup>, D. Schumann<sup>ag</sup>, A. Sekhar<sup>l</sup>, A. G. Smith<sup>l</sup>,  
 N. V. Sosnin<sup>ap</sup>, M. E. Stamati<sup>ah,g</sup>, A. Sturniolo<sup>x</sup>, G. Tagliente<sup>z</sup>, A. Tarifeño-Saldivia<sup>r</sup>,  
 D. Tarrío<sup>ay</sup>, P. Torres-Sánchez<sup>aj</sup>, S. Urlass<sup>n,g</sup>, E. Vagena<sup>ah</sup>, S. Valenta<sup>ao</sup>, V. Variale<sup>z</sup>, P. Vaz<sup>af</sup>,  
 G. Vecchio<sup>j</sup>, D. Vescovi<sup>ad</sup>, V. Vlachoudis<sup>g</sup>, R. Vlastou<sup>w</sup>, A. Wallner<sup>n</sup>, P. J. Woods<sup>ap</sup>, T. Wright<sup>l</sup>,  
 R. Zarrella<sup>t,aq</sup>, P. Žugec<sup>p</sup>

<sup>a</sup> Centro de Investigaciones Energéticas Medioambientales y Tecnológicas (CIEMAT), Spain

<sup>b</sup> University of Lodz, Poland

\* Corresponding author.

E-mail addresses: [adrian.sanchez@ciemat.es](mailto:adrian.sanchez@ciemat.es) (A. Sánchez-Caballero), [daniel.cano@ciemat.es](mailto:daniel.cano@ciemat.es) (D. Cano-Ott), [emilio.mendoza@ciemat.es](mailto:emilio.mendoza@ciemat.es) (E. Mendoza).

<https://doi.org/10.1016/j.physletb.2025.140070>

Received 20 May 2025; Received in revised form 6 November 2025; Accepted 26 November 2025

Available online 5 December 2025

0370-2693/© 2025 The Author(s). Published by Elsevier B.V. Funded by SCOAP<sup>3</sup>. This is an open access article under the CC BY license (<http://creativecommons.org/licenses/by/4.0/>).

- <sup>c</sup> NACP–Nuclear Data Section, International Atomic Energy Agency, A-1400 Vienna, Austria  
<sup>d</sup> SCK CEN, Belgian Nuclear Research Centre, Boeretang 200, Mol, B-2400, Belgium  
<sup>e</sup> European Commission, Joint Research Centre (JRC), Geel, Belgium  
<sup>f</sup> CEA, DEN, DER, SPRC, Cadarache, 13108 Saint-Paul-lès-Durance, France  
<sup>g</sup> European Organization for Nuclear Research (CERN), Switzerland  
<sup>h</sup> Istituto Nazionale di Fisica Nucleare, Sezione di Pavia, Italy  
<sup>i</sup> Department of Physics, University of Pavia, Italy  
<sup>j</sup> INFN Laboratori Nazionali del Sud, Catania, Italy  
<sup>k</sup> Instituto de Física Corpuscular, CSIC - Universidad de Valencia, Spain  
<sup>l</sup> University of Manchester, UK  
<sup>m</sup> CEA Irfu, Université Paris-Saclay, F-91191 Gif-sur-Yvette, France  
<sup>n</sup> Helmholtz-Zentrum Dresden-Rossendorf, Germany  
<sup>o</sup> Horia Hulubei National Institute of Physics and Nuclear Engineering, Romania  
<sup>p</sup> Department of Physics, Faculty of Science, University of Zagreb, Zagreb, Croatia  
<sup>q</sup> University of Santiago de Compostela, Spain  
<sup>r</sup> Universitat Politècnica de Catalunya, Spain  
<sup>s</sup> Agenzia nazionale per le nuove tecnologie, l'energia e lo sviluppo economico sostenibile (ENEA), Italy  
<sup>t</sup> Istituto Nazionale di Fisica Nucleare, Sezione di Bologna, Italy  
<sup>u</sup> Istituto Nazionale di Fisica Nucleare, Sezione di Trieste, Italy  
<sup>v</sup> Department of Physics, University of Trieste, Italy  
<sup>w</sup> National Technical University of Athens, Greece  
<sup>x</sup> Istituto Nazionale di Fisica Nucleare, Sezione di Torino, Italy  
<sup>y</sup> Department of Physics, University of Torino, Italy  
<sup>z</sup> Istituto Nazionale di Fisica Nucleare, Sezione di Bari, Italy  
<sup>aa</sup> Universidad de Sevilla, Spain  
<sup>ab</sup> Istituto Nazionale di Fisica Nucleare, Sezione di Perugia, Italy  
<sup>ac</sup> Istituto Nazionale di Astrofisica - Osservatorio Astronomico d'Abruzzo, Italy  
<sup>ad</sup> Goethe University Frankfurt, Germany  
<sup>ae</sup> Physikalisch-Technische Bundesanstalt (PTB), Bundesallee 100, Braunschweig, 38116, Germany  
<sup>af</sup> Instituto Superior Técnico, Lisbon, Portugal  
<sup>ag</sup> Paul Scherrer Institut (PSI), Villigen, Switzerland  
<sup>ah</sup> University of Ioannina, Greece  
<sup>ai</sup> Affiliated with an institute covered by a cooperation agreement with CERN,  
<sup>aj</sup> University of Granada, Spain  
<sup>ak</sup> Istituto Nazionale di Fisica Nucleare, Sezione di Roma1, Roma, Italy  
<sup>al</sup> University of York, United Kingdom,  
<sup>am</sup> TU Wien, Atominstytut, Stadionallee 2, 1020, Wien, Austria  
<sup>an</sup> Japan Atomic Energy Agency (JAEA), Tokai-Mura, Japan  
<sup>ao</sup> Charles University, Prague, Czech Republic  
<sup>ap</sup> School of Physics and Astronomy, University of Edinburgh, UK  
<sup>aq</sup> Dipartimento di Fisica e Astronomia, Università di Bologna, Italy  
<sup>ar</sup> INFN Laboratori Nazionali di Legnaro, Italy  
<sup>as</sup> Dipartimento Interateneo di Fisica, Università degli Studi di Bari, Italy  
<sup>at</sup> Consiglio Nazionale delle Ricerche, Bari, Italy  
<sup>au</sup> Dipartimento di Fisica e Geologia, Università di Perugia, Italy  
<sup>av</sup> INFN Laboratori Nazionali di Frascati, Italy  
<sup>aw</sup> Istituto Nazionale di Fisica Nucleare, Sezione di Catania, Italy  
<sup>ax</sup> Department of Physics and Astronomy, University of Catania, Italy  
<sup>ay</sup> Department of Physics and Astronomy, Uppsala University, Box 516, 75120, Uppsala, Sweden

## ARTICLE INFO

Editor: Prof. Betram Blank

## Keywords:

Nuclear reaction  
 Neutron-induced reaction  
 n\_TOF  
 Fission  
 Cross section measurement  
 Plutonium-239

## ABSTRACT

The  $^{239}\text{Pu}(n,f)$  cross section was measured with uncertainties below 4% from 20 meV up to 10 MeV of neutron energy at CERN's n\_TOF facility using a novel fission fragment detector with a 185.59 m flight path. Measured cross section was normalized to 1059(6) eV·b in the 9–20 eV energy range, and is consistent within uncertainties with the standard thermal value and the IAEA reference  $^{239}\text{Pu}(n,f)$  cross section. Experimental key values include the integral ratio  $I_3/I_1 = 41.20(42)$  defined by Duran et al. 2024 and the spectrum averaged cross section in  $^{252}\text{Cf}(sf)$  reference neutron field of 1802(40) mb.

## 1. Introduction

The neutron-induced fission cross section of  $^{239}\text{Pu}$  plays a key role in the design and operation of multiple types of nuclear reactors [1]. In addition, it is also crucial for a safe and efficient management of nuclear waste, including partitioning and transmutation processes [2, 3]. In addition, accurate prediction of fuel depletion and subsequent loss of reactivity in power reactors is vital for fuel management and determining the operating cycle length in commercial reactors, which has significant economic implications.

The nuclear power industry was generally satisfied with the performance of the JEFF-3.1.1 [4] library (industry reference in Europe) and the ENDF/B-VII.1 [5] library (industry reference in the US). However, it was found that the loss of reactivity with fuel burn-up is significantly

larger with the newer JEFF-3.3 [6] and ENDF/B-VIII.0 [7] cross section data compared to the industry reference libraries. This issue led to numerous studies that highlighted the importance of the  $^{239}\text{Pu}$  resonance cross sections in reactivity as a function of burn-up, and the critical need for high-quality  $^{239}\text{Pu}$  capture and fission cross sections below 5 eV for nuclear power applications.

In addition, many fission cross section measurements [8–10] over the years used the  $^{239}\text{Pu}(n,f)$  cross section as a reference for fast neutron energies. Therefore, it is necessary to continue to update this reference cross section evaluated by the Neutron Data Standards (NDS) [11].

Since the mid-20th century, various techniques have been employed to measure the  $^{239}\text{Pu}$  neutron-induced fission cross section [12–28]. The time-of-flight (TOF) method was commonly used because it enables determining the incident neutron energy in a broad range on the basis

of the neutron travel time from the generation point to the target. Weston et al. used the TOF method, covering a wide neutron energy range between 2 meV and 20 MeV, in the 20 m and 86 m flight paths at Oak Ridge National Laboratory to undertake several high-resolution measurements [25–28]. Tovesson et al. [29], at Los Alamos Neutron Science Center (LANSCE), conducted two measurements with a 99.1 % purity sample at different target stations. At the Lujan center, neutron energies from 10 meV to 200 keV were measured utilizing a 7.93 m flight path. At the Weapon Neutron Research (WNR) facility, energies from 200 keV to 200 MeV were measured utilizing a 10 m flight path. The most recent measurements include an experiment performed at the China Spallation Neutron Source by Qiu et al. [30] in the range from 4 keV to 100 MeV, a measurement by Pérez Sánchez et al. [31] at the ALTO facility in Orsay via a surrogate reaction, and two new measurements by Snyder et al. [32] and Dongwi et al. [33] with a Time Projection Chamber at a 10 m flight path at LANSCE, reporting uncertainties below 1 % in the  $^{239}\text{Pu}(n,f)/^{235}\text{U}(n,f)$  ratio, for neutron energies between 0.1 MeV and 100 MeV.

No other measurement has ever spanned the extensive energy range from the thermal point up to 10 MeV. This is because it is technically very challenging to design and optimize an experimental setup that achieves both low uncertainty and high-energy resolution across such a broad energy range.

We introduce here the first measurement of the  $^{239}\text{Pu}(n,f)$  cross section, which covers neutron energies from 20 meV to 10 MeV. Minimal corrections were required due to the outstanding features of the experimental setup and the samples used. The measurement was performed at n\_TOF [34–36], the neutron TOF facility at CERN. Our results demonstrate unprecedented consistency and low uncertainties across the entire covered energy range, in agreement with many previous experiments conducted at different energy ranges.

## 2. Experiment

The n\_TOF pulsed neutron beam is generated by spallation of 7 ns (RMS) wide proton bunches in a gas-cooled lead target [37,38]. The measurement was carried out in the first experimental area (EAR1), which is located approximately 185 meters from the neutron source in the horizontal direction. Such a long flight path makes n\_TOF an appropriate facility for measuring cross sections with a very high neutron energy resolution, ranging from a  $\Delta E_n/E_n$  value of 0.03 % at 1 eV to 0.5 % around 1 MeV [39]. Neutrons emerging from the spallation target are moderated by a 4 cm layer of borated water, producing a white neutron spectrum from about 20 meV up to a few GeV [40]. Subsequently, the beam pulse is stripped of charged particles by a sweeping magnet and shaped by two collimators.

Ten  $^{239}\text{Pu}$  thin samples were produced and assembled inside a multi-section ionization chamber at the JRC-Geel Target Preparation laboratory [41]. The Pu material had an amount of  $^{239}\text{Pu}$  of 99.90 % (see Table 1), and was purified from  $^{241}\text{Am}$  by anion exchange at SCK CEN Belgium [42] removing the presence of any significant background related to contaminants in fission measurement.

**Table 1**

Isotopic abundances of the plutonium used for the samples, determined by thermal ionization mass spectrometry at JRC Geel in 2017.

Isotope	Amount fraction (%)
$^{239}\text{Pu}$	99.90259(14)
$^{240}\text{Pu}$	0.05818(4)
$^{241}\text{Pu}$	0.02501(5)
$^{242}\text{Pu}$	0.01288(7)
$^{238}\text{Pu}$	<0.0002
$^{244}\text{Pu}$	<0.0002

The samples, with a total mass of about 9 mg, included nine samples of approximately 1 mg (about 300  $\mu\text{g}/\text{cm}^2$  of areal density) each and one sample of 0.1 mg. The latter, with an areal density of about 40  $\mu\text{g}/\text{cm}^2$ , was manufactured with the aim of minimizing the absorption of fission fragments within the sample, i.e., to maximize detection efficiency. Thin samples also minimize the need for multiple scattering corrections. The samples were prepared by molecular plating the Pu material on 10  $\mu\text{m}$  thick aluminum foils [43]. They were deposited using a circular mask with an inner diameter of 2 cm at the center of the aluminum backing.

The Fission Fragment Detector (FFD) [41], used in this work, consists of ten independent parallel plate ionization chambers, each made of an aluminum anode separated by 4.5 mm from the cathode that contains the  $^{239}\text{Pu}$  samples. Constantly flowing through the space between the electrodes, a gas mixture of 90 % Ar and 10 %  $\text{CF}_4$  at atmospheric pressure becomes ionized when fission fragments are emitted from the  $^{239}\text{Pu}$  samples. The detector was optimized to provide fast signals with 40 ns rise time and a high detection efficiency of 89.4(5)%. The signals were digitized using the n\_TOF data acquisition system [44] and analyzed offline with a dedicated pulse shape analysis routine, particularly developed for this challenging measurement. The FFD was operated simultaneously with a  $\gamma$ -ray detector, the n\_TOF Total Absorption Calorimeter (TAC) [45], in an experimental campaign dedicated to measure the neutron-induced fission, capture and fission-to-capture ratio (also called  $\alpha$ -ratio) of  $^{239}\text{Pu}$ , using a similar technique as in Balibrea-Correa et al. [46], Guerrero et al. [47], Bacak, M. et al. [48].

The distribution of the ten parallel plutonium samples covered a distance of 6.45 cm along the neutron beam axis. The time of flight of the signals from the ten ionization chambers has been corrected according to this space distribution of samples, using the fifth sample as the reference. As a result, an effective time-of-flight distance of 185.59(1) m is used. The exact value was found by adjusting the position of the fission resonances to the  $^{239}\text{Pu}(n,f)$  evaluation of the ENDF/B-VIII.0 nuclear data library.

## 3. Analysis

The design of the FFD and the properties of the selected ionization gas ensure an excellent separation between  $\alpha$  particles and fission fragments using the signal amplitude. This is particularly important since the  $\alpha$ -activity of  $^{239}\text{Pu}$  is around 2 MBq/mg, which results in a counting rate in each of the ten detectors of about 1 count/ $\mu\text{s}$ , which is  $10^2$ - $10^5$  larger than the fission-fragment counting rate, depending on the TOF. This excellent separation is shown in Fig. 1, where the amplitude spectrum measured in the vicinity of the strongest resonance of  $^{239}\text{Pu}$  at 0.3 eV, in red, is compared with the spectrum measured in the absence of the beam, in blue. The spectrum associated with fission fragments appears clearly separated from the contribution of  $\alpha$ -particles, allowing the isolation of fission fragment signals by applying an amplitude threshold, represented by the vertical dashed line in Fig. 1. The choice of this threshold ensures that nearly all fission fragments are selected, while the number of high-amplitude signals from alpha particles remains negligible.

The  $^{239}\text{Pu}(n,f)$  reaction yield,  $Y_f$ , has been obtained according to:

$$Y_f(E_n) = N_f \frac{C_{\text{FF}}(E_n)}{\varphi_{2\text{cm}}(E_n)}, \quad (1)$$

where  $N_f$  is a normalization factor independent of the neutron energy  $E_n$ ,  $C_{\text{FF}}(E_n)$  are the counts in the FFD using the threshold for the fission fragments, and  $\varphi_{2\text{cm}}(E_n)$  is the shape of the neutron fluence that crosses a 2 cm diameter sample as a function of  $E_n$ .

The n\_TOF neutron fluence as a function of energy is derived from dedicated measurements using different detectors based on the standard reactions  $^6\text{Li}(n,t)^4\text{He}$ ,  $^{10}\text{B}(n,\alpha)^7\text{Li}$ , and  $^{235}\text{U}(n,f)$  [11]. The beam characterization process (energy, time, and spatial distribution) includes both experimental data and Monte Carlo simulations performed with FLUKA [40,49–53]. The simulations are validated against experimental

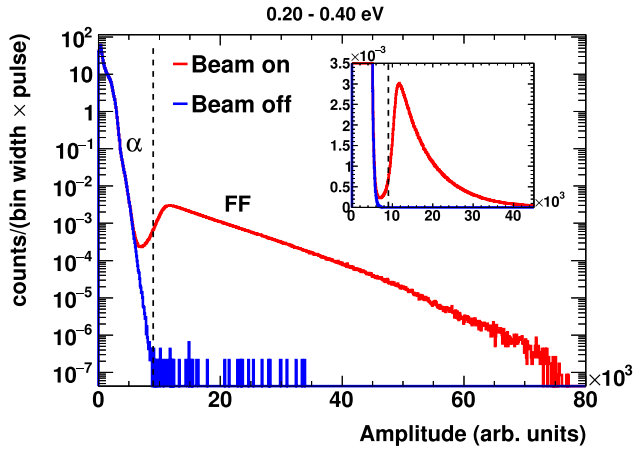


Fig. 1. Amplitude spectra obtained with the FFD for beam-on and beam-off measurements, showing the separation between alpha particles ( $\alpha$ ) and fission fragments (FF). The inset displays a zoom to the FF peak in linear scale.

data and allow for a complete beam characterization, which would be virtually impossible to achieve with experimental measurements alone.

This process results in the *evaluated* neutron fluence  $\phi_{\text{eval}}(E_n)$ . In practice, the fluence was further monitored throughout the entire  $^{239}\text{Pu}$  campaign with four silicon detectors (SiMon [54]) through the  $^6\text{Li}(n,t)^4\text{He}$  standard reaction, obtaining values compatible with those of the evaluated fluence. All detectors used to obtain  $\phi_{\text{eval}}(E_n)$  covered the entire beam, while the  $^{239}\text{Pu}$  samples covered only a fraction of the beam. Therefore, the energy dependence of  $\varphi_{2\text{cm}}(E_n)$  is different from the energy dependence of  $\phi_{\text{eval}}(E_n)$ , especially below 0.1 eV and above 1 MeV.

For low neutron energies, below 0.1 eV, the  $\varphi_{2\text{cm}}(E_n)$  fluence correction was determined by measuring the  $^{197}\text{Au}(n,\gamma)$  cross section with a gold sample of the same size as the plutonium samples with the TAC. Above 0.1 eV, the fluence correction was derived from the beam characterization with FLUKA mentioned above. The resulting corrections on the energy dependence of the neutron fluence remain below 2% in the 0.1– $10^5$  eV energy range, 2–9% in the 0.1–1 MeV range, and 8–34% in the 1–10 MeV region.

The shape of neutron fluence  $\varphi_{2\text{cm}}(E_n)$  can be seen as the gray curve in Fig. 2. The high instantaneous neutron fluence at n\_TOF, combined with the large  $^{239}\text{Pu}(n,f)$  cross section, ensures sufficient counting statistics to measure data from 20 meV up to about 10 MeV.

The uncertainties in the  $^{239}\text{Pu}(n,f)$  yield due to systematic effects are those of  $\varphi_{2\text{cm}}(E_n)$ , shown in Fig. 2, plus the uncertainty in normalization.

#### 4. Results and discussion

The (n,f) detection efficiency was assumed to be constant over the measured neutron energy range. The impact on efficiency due to the kinematic boost of the fissioning nucleus and the fragment angular

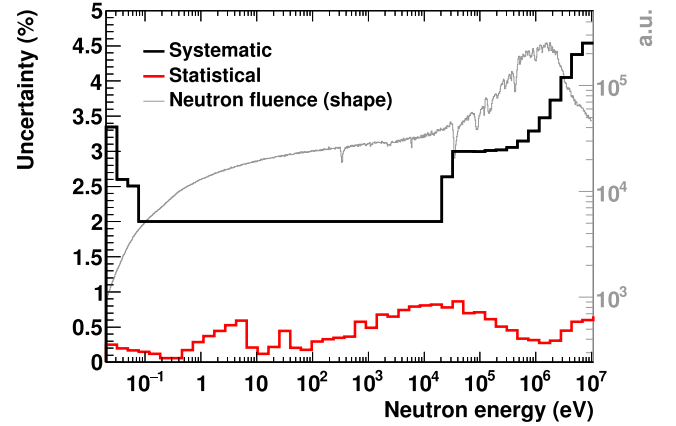


Fig. 2. Uncertainties in the  $^{239}\text{Pu}(n,f)$  yield due to counting statistics (*Statistical*) and due to systematic effects (*Systematic*) excluding normalization, when using 5 bins per decade. The neutron fluence  $\phi_{2\text{cm}}(E_n)$  is also shown (right axis scale).

anisotropy, both energy dependent [32,59], are minimal in the present experimental setup, as the plutonium deposits and active volumes are alternated between the upstream and downstream sides of the backing foil [41]. To prove this, the energy dependence of the counting rates from upstream and downstream samples was compared, revealing only a small deviation of 1–2% over the 100 keV–10 MeV range. When the count rates from all samples are combined, these small variations are expected to average out, leading to an efficiency correction that is negligible, on the order of a few per thousand, and well within the estimated uncertainties due to systematic effects.

Consequently, the efficiency can be absorbed into the normalization constant  $N_f$  in Eq. (1). This value is calculated by normalizing the  $^{239}\text{Pu}(n,f)$  cross section integral in the 9–20 eV region (defined as  $I_3$  [55]) to the value of  $1059(6)$  eV · b recommended by Duran et al. [55] to normalize the time-of-flight experiments to measure  $^{239}\text{Pu}(n,f)$  cross sections. Using this normalization, the uncertainties due to the detection efficiency, as well as the mass of the samples and the absolute value of the neutron fluence, are removed. The authors in [55] also provide recommended values for the integral in the 0.02–0.06 eV interval ( $I_1$ ) and for the ratio  $I_3/I_1$ . A comparison of these integrals for the n\_TOF measured data with those derived from the selected evaluations is shown in Table 2.

Good agreement within uncertainties is observed in the ratio of cross section integrals  $I_3/I_1 = 41.65(22)$  recommended by Duran et al. [55] with the value of  $41.20(42)$  measured in this work. This integral ratio is independent of normalization, providing a proof of the consistency of the measured cross section shape in the thermal and resonance region below 20 eV. Using the  $I_3$  normalization, we observe a 1% overestimation of the  $I_1$  integral, as shown in Table 2. An additional neutron energy interval from 8–10 MeV defines the integral  $I_{\text{HE}}$  recommended in a recent work [56]. This integral value is used to compare measured

Table 2

Ratio of integrals  $I_1$  and  $I_3$  [55], and  $I_{\text{HE}}$  [56] using the n\_TOF  $^{239}\text{Pu}(n,f)$  cross section data to the corresponding evaluated values for the same integrals from refs. [6,7,11,55,58]. The uncertainties due to statistics and systematic effects for each value are shown in the first and second number in parenthesis, respectively.

	$I_1(0.02\text{--}0.06\text{ eV})$	$I_3(9\text{--}20\text{ eV})$	$I_3/I_1$	$I_{\text{HE}}(8\text{--}10\text{ MeV})$
n_TOF/1. Durán et al. [55,56]	1.011(1)(29)	1.0	0.989(2)(20)	1.014(8)(46)
n_TOF/ENDF/B-VIII.1 [57]	1.014(1)(29)	1.010(1)(20)	0.995(2)(20)	1.007(8)(46)
n_TOF/ENDF/B-VIII.0 [7]	1.013(1)(29)	1.007(1)(20)	0.994(2)(20)	1.016(8)(46)
n_TOF/JEFF-3.3 [6]	1.015(1)(29)	0.986(1)(20)	0.972(2)(20)	1.011(8)(46)
n_TOF/ $\sigma_f$ ref. (NDS [11])	–	–	–	1.016(8)(46)

**Table 3**

$^{239}\text{Pu}(n,f)$  SACS in the  $^{252}\text{Cf}(sf)$  reference neutron field [63–65] derived from n\_TOF experimental data is compared with the value derived from the IAEA reference cross section [11], and with evaluations based on direct SACS experimental data ([62,67]). Total SACS uncertainties are reported. Note that the SACS uncertainty derived in this work is dominated by systematic effects (3.6%) over the statistical ones (just 0.13%).

Data	$^{239}\text{Pu}(n,f)$ SACS in $^{252}\text{Cf}(sf)$ (millibarn)
Derived, this work	$1802 \pm 65$ (3.6%)
Derived, IAEA standard 2017 [11]	$1798 \pm 23$ (1.3%)
Mannhart evaluation [67]	$1812 \pm 25$ (1.4%)
Capote et al. evaluation [62]	$1826 \pm 19$ (1.0%)

and evaluated data with standard and/or reference cross sections for very fast neutrons, and is also shown in Table 2. The integral  $I_{\text{HE}}$  derived from the new n\_TOF data agrees with all evaluations within quoted uncertainties; the best agreement is reached for the recent evaluation by the International Nuclear Data Evaluation Network (INDEN) [60], released in August 2023. The INDEN evaluation in the fast neutron region was the latest iteration of the gmapy fit undertaken by the Neutron Standard Committee [61,62] and was adopted for the ENDF/B-VIII.1 file [57,58]. The agreement of cross section integrals across different energy ranges discussed above confirms the reliability and robustness of the present data in the thermal, epithermal, and fast regions, covering all energy domains relevant to nuclear reactors.

#### 4.1. Spectrum averaged cross section

The broad coverage of neutron energy in this work enables the calculation of the spectrum average cross section (SACS) of the  $^{239}\text{Pu}(n,f)$  reaction in the  $^{252}\text{Cf}(sf)$  reference neutron field [63–65], a very important quantity to normalize cross section data in the neutron standard evaluation [11]. The SACS value calculated with the n\_TOF  $^{239}\text{Pu}$  fission data is compared in Table 3 with the value derived from the IAEA  $^{239}\text{Pu}(n,f)$  reference cross section of NDS [11]. Evaluated SACS by Mannhart [67] and Capote et al. [62], which are based on direct integral cross section measurements, are also shown for comparison. These evaluated values show full compatibility with our result within reported uncertainties. SACS values in the  $^{252}\text{Cf}(sf)$  neutron field are especially sensitive to the data in the 0.1–5 MeV energy region where the  $^{252}\text{Cf}(sf)$  spectrum reaches its maximum probability. This energy region corresponds to the first-chance neutron fission on actinides. The excellent agreement observed between the SACS derived in this work and the one obtained from the IAEA standard fit [11] also shows the consistency of the n\_TOF measured cross section using Duran's normalization [55] in the 9–20 eV energy region [55] with the IAEA reference cross section in the fast neutron region.

#### 4.2. Comparison with experimental and evaluated data

The measured high resolution n\_TOF  $^{239}\text{Pu}(n,f)$  yield from 16 keV up to 22 keV in the unresolved resonance region (URR) is compared to previous data and evaluations in Fig. 3(a). The IAEA reference cross section [11] (adopted by the ENDF/B-VIII.0 [7]) uses a low-density energy grid at these neutron energies (blue curve), so it only describes the high-resolution experimental data on average. The ENDF/B-VIII.1 evaluation (dashed line) is based on the Weston data [27] and shows good agreement with the n\_TOF data up to about 20 keV (which is the upper limit of the Weston data [27]). The measured fluctuations of the cross section in the Weston and n\_TOF data are in perfect agreement. The new n\_TOF data could be used to extend such fluctuations in evaluations above 20 keV, which may be important for the criticality of intermediate spectrum assemblies. A comparison of selected EXFOR data with the n\_TOF  $^{239}\text{Pu}(n,f)$  fast neutron yield from 200 keV up to 10 MeV

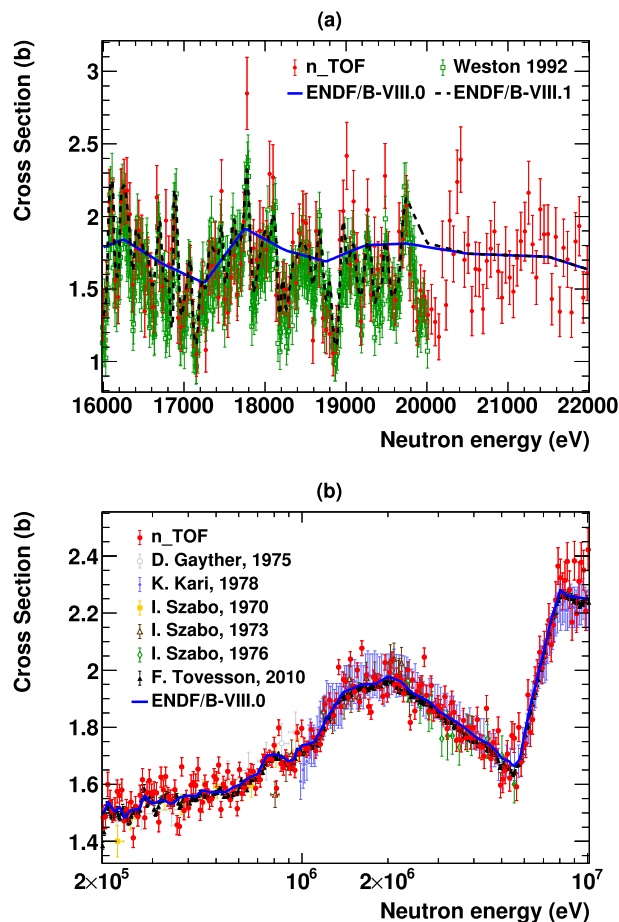


**Fig. 3.** The n\_TOF measured  $^{239}\text{Pu}(n,f)$  cross section compared to selected experimental and evaluated data. Error bars show either statistical uncertainties when specified in the EXFOR files or total uncertainties otherwise. (a) Comparison to Weston [27], the IAEA reference cross section [11] taken from ENDF/B-VIII.0 [7], and the ENDF/B-VIII.1 [57] evaluation in the energy range 16–22 keV. (b) Comparison to selected EXFOR data and to the IAEA reference cross section [11] taken from ENDF/B-VIII.0 [7] in the energy range from 200 keV up to 10 MeV.

is shown in Fig. 3(b); a good agreement is observed between all data as well as with the IAEA reference cross section [11] adopted by the ENDF/B-VIII.0 evaluation.

The experimental fission yield, integrated with 100 bins per decade, for the entire neutron energy range from 20 meV to 10 MeV is shown in Fig. 4(a). The fission yields calculated from the ENDF/B-VIII.0, ENDF/B-VIII.1 and JEFF-3.3 nuclear data libraries, taking into account the effects of the n\_TOF resolution function and sample thickness, are also shown for comparison. The ratios shown in the bottom strip of Fig. 4(a) are calculated relative to the ENDF/B-VIII.1 data, with error bars showing only uncertainties due to counting statistics. Good agreement with the evaluations is generally observed, but deviations are observed in the resonance region above 5 eV and continue up to 100 keV.

The observed agreement can be better visualized in Fig. 4(b), which shows the integral ratios over broader energy bins of n\_TOF relative to the selected evaluations. The energy bins used for the integration are close to one bin per decade to reduce the spread of experimental data.

The integral values measured deviate from all the evaluations by less than 1% above 10 keV (in the fast neutron range). However, a larger discrepancy of about 4% is observed with JEFF-3.3 between 200 meV and 20 eV, and with the ENDF/B-VIII.1 evaluation in the 100 eV to 10 keV region. The best agreement below 5 eV, a region of greatest relevance

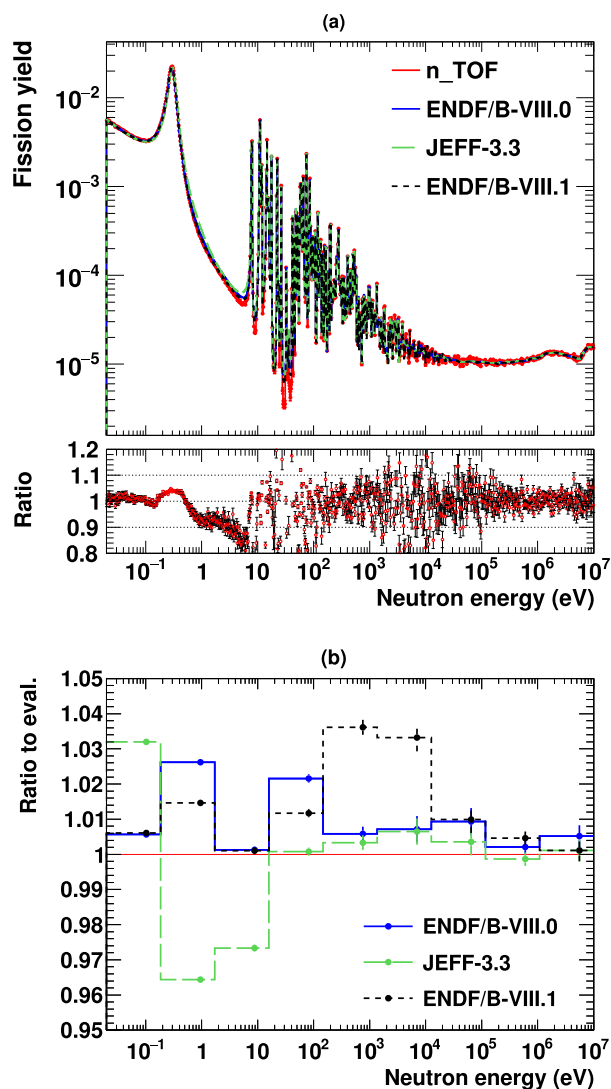


Fig. 4. The  $n_{\text{TOF}}$  measured  $^{239}\text{Pu}(n,f)$  yield from 20 meV up to 10 MeV compared to selected evaluated data [6,7,57]. Error bars indicate only uncertainties due to counting statistics. (a) Integration with 100 bins per decade. Ratios of experimental data relative to ENDF/B-VIII.1 are shown. (b) Ratios of  $n_{\text{TOF}}$  data to individual evaluations at approximately 1 bin per decade.

for the nuclear energy industry, is shown with the  $^{239}\text{Pu}(n,f)$  evaluation by INDEN [60], which has been adopted by the nuclear data library ENDF/B-VIII.1 [57,58]. All evaluations require further refinement considering our new data.

## 5. Summary and conclusions

The  $^{239}\text{Pu}(n,f)$  cross section has been measured at the high-resolution time-of-flight facility at CERN ( $n_{\text{TOF}}$ ) with uncertainties lower than 4%, for the first time covering nearly nine orders of magnitude in neutron incident energy from 0.02 eV to 10 MeV in one single measurement. The utilization of thin highly-enriched plutonium samples, a novel fast fission fragment detector with minimal background, and the exceptional characteristics of the  $n_{\text{TOF}}$  neutron beam pulses has led to the creation of a new high-quality experimental dataset. The integrated experimental  $^{239}\text{Pu}(n,f)$  fission yield generally agrees well with the major evaluations and Neutron Standards. The new measured data below 5 eV satisfies the target accuracy requirements for nuclear power applications in that energy region. The high neutron-energy resolution can provide valuable

information on the shape of resonances, contributing to the refinement of future evaluations in the resolved resonance region. Furthermore, the use of newly measured data will lead to further improvement of the IAEA  $^{239}\text{Pu}(n,f)$  reference cross section and future evaluations, supporting the advancement of nuclear energy as a carbon-free source.

## Data availability

Data will be made available on request.

## Declaration of competing interest

The authors declare that they have no known competing financial interests or personal relationships that could have appeared to influence the work reported in this paper.

## Acknowledgements

In memory of Koen Vanaken, whose invaluable contributions and dedication to the Fuel Materials laboratories of SCK CEN will always be remembered. We wish to acknowledge André Moens (formerly member of the JRC-Geel Target Preparation laboratory, now retired) for his important contribution to the preparation of the  $^{239}\text{Pu}$  samples. Funding for this project was provided by the Euratom research and training program 2014–2018 under grant agreement no 847594 (ARIEL). Additional support came from the European Commission through the H2020 Framework Programme under grant agreement no 847552 (SANDA) and the project 36225/2/2021-1-RD-EUFRACT-GELINA (CHARPU), as well as from I + D + i grants PGC2018-096717-B-C21, PID2021-123100NB-I00, PID2022-142589OB-I00, and PDC2021-120828-I00 funded by MCIN/AEI/10.13039/501100011033. Furthermore, this research received partial funding from the National Science Centre in Poland (grant no UMO-2021/41/B/ST2/00326). The support of the funding agencies of all other participating institutes is also appreciated.

## References

- [1] N. Colonna, F. Belloni, E. Berthoumieux, M. Calviani, C. Domingo-Pardo, C. Guerrero, D. Karadimos, C. Lederer, C. Massimi, C. Paradela, R. Plag, J. Praena, R. Sarmiento, Advanced nuclear energy systems and the need of accurate nuclear data: the  $n_{\text{TOF}}$  project at CERN, *Energy Environ. Sci.* 3 (2010) 1910–1917. <https://doi.org/10.1039/C0EE00108B>
- [2] M. Salvatores, G. Palmiotti, Radioactive waste partitioning and transmutation within advanced fuel cycles: achievements and challenges, *Prog. Part. Nucl. Phys.* 66 (1) (2011) 144–166. <https://doi.org/10.1016/j.pnpnp.2010.10.001>
- [3] G. Aliberti, G. Palmiotti, M. Salvatores, T.K. Kim, T.A. Taiwo, M. Anitescu, I. Kodeli, E. Sartori, J.C. Bosq, J. Tommasi, Nuclear data sensitivity, uncertainty and target accuracy assessment for future nuclear systems, *Ann. Nucl. Energy* 33 (8) (2006) 700–733. <https://doi.org/10.1016/j.anucene.2006.02.003>
- [4] A. Santamarina, et al., The JEFF-3.1.1 nuclear data library, *Technical Report 10.2, NEA*, 2009.
- [5] M.B. Chadwick, et al., ENDF/B-VII.1 nuclear data for science and technology: cross sections, covariances, fission product yields and decay data, *Nucl. Data Sheet.* 112 (12) (2011) 2887–2996. Special Issue on ENDF/B-VII.1 Library, <https://doi.org/10.1016/j.nds.2011.11.002>
- [6] A.J.M. Plompen, et al., The joint evaluated fission and fusion nuclear data library, JEFF-3.3, *Eur. Phys. J. A* 56 (2020) 1–108.
- [7] D.A. Brown, et al., ENDF/B-VIII.0: The 8th major release of the nuclear reaction data library with CIELO-project cross sections, new standards and thermal scattering data, *Nucl. Data Sheet.* 148 (2018) 1–142. Special Issue on Nuclear Reaction Data, <https://doi.org/10.1016/j.nds.2018.02.001>
- [8] V.M. Kupriyanov, B.I. Fursov, V.I. Ivanov, G.N. Smirenkin, Measurement of the  $^{237}\text{Np}/^{239}\text{Pu}$  and  $^{241}\text{Am}/^{239}\text{Pu}$  cross section ratios for 0.13–7.0 MeV neutrons, *Sov. Atom. Energy* 45 (1978) 1176. <http://dx.doi.org/10.1007/BF01181116>
- [9] B.I. Fursov, E.Y. Baranov, M.P. Klemyshev, B.F. Samylin, G.N. Smirenkin, Y.M. Turchin, Measurement of the fast-neutron fission cross section of  $^{231}\text{Pa}$  and  $^{243}\text{Am}$ , *Sov. Atom. Energy* 59 (1985) 899. <http://dx.doi.org/10.1007/BF01133085>
- [10] B.I. Fursov, E.Y. Baranov, M.P. Klemyshev, B.F. Samylin, G.N. Smirenkin, Y.M. Turchin, Measurement of the fission cross section of  $^{232}\text{U}$  for neutron energies in the range 0.06–7.40 MeV, *Sov. Atom. Energy* 61 (1986) 963. <http://dx.doi.org/10.1051/epjconf/202328100027>
- [11] A.D. Carlson, V.G. Pronyaev, R. Capote, G.M. Hale, Z.-P. Chen, I. Duran, F.-J. Hambach, S. Kunieda, W. Mannhart, B. Marcinkevicius, et al., Evaluation of the neutron data standards, *Nucl. Data Sheet.* 148 (2018) 143–188. <https://doi.org/10.1016/j.nds.2018.02.002>

- [12] L.M. Bollinger, R.E. Cote, G.E. Thomas, The slow neutron cross sections of plutonium-239, in: *Second Internat. At. En. Conf. Series Geneva*, 15, 1958, p. 127.
- [13] J.A. Farrell, G.F. Auchampaugh, M.S. Moore, P.A. Seeger, A simultaneous measurement of the fission, capture, scattering and total cross-sections of  $^{239}\text{Pu}$ , in: *Nuclear Data for Reactors. Proceedings of the Second International Conference*, Vol. 1, Helsinki, 1970, p. 543.
- [14] G.W. Carlson, J.W. Behrens, Measurement of the fission cross sections of uranium-233 and plutonium-239 relative to uranium-235 from 1 keV to 30 MeV, *Nucl. Sci. Eng.* 66 (2) (1978) 205–216.
- [15] R. Gwin, L.W. Weston, G. De Saussure, R.W. Ingle, J.H. Todd, F.E. Gillespie, R.W. Hockenbury, R.C. Block, Simultaneous measurement of the neutron fission and absorption cross sections of Plutonium-239 over the energy region 0.02 eV to 30 keV, *Nucl. Sci. Eng.* 45 (1) (1971) 25–36.
- [16] W.K. Lehto, Fission cross-section ratio measurements of  $^{239}\text{Pu}$  and  $^{235}\text{U}$  to  $^{235}\text{U}$  from 0.24 to 24 keV, *Nucl. Sci. Eng.* 39 (3) (1970) 361–367.
- [17] R. Gwin, E.G. Silver, R.W. Ingle, H. Weaver, Measurement of the neutron capture and fission cross sections of  $^{239}\text{Pu}$  and  $^{235}\text{U}$ , 0.02 eV to 200 keV, the neutron capture cross sections of  $^{197}\text{Au}$ , 10 to 50 keV, and neutron fission cross sections of  $^{235}\text{U}$ , 5 to 200 keV, *Nucl. Sci. Eng.* 59 (2) (1976) 79–105.
- [18] I. Szabo, G. Filippi, J.L. Huet, J.L. Leroy, J.P. Marquette, New absolute measurement of the neutron-induced fission cross section of  $^{235}\text{U}$ ,  $^{239}\text{Pu}$ , and  $^{241}\text{Pu}$  from 17 keV to 1 MeV, Technical Report, Commissariat à l'Énergie Atomique, Cadarache (France), 1971.
- [19] I. Szabo, G. Filippi, J.L. Huet, J.L. Leroy, J.P. Marquette,  $^{235}\text{U}$  fission cross section from 10 keV to 200 keV, in: *Proceedings of the Third Conference on Neutron Cross Sections and Technology*, Knoxville, 15, 2, 1971, pp. 573–583.
- [20] I. Szabo, J.L. Leroy, J.P. Marquette, Absolute measurement of fission cross-sections of  $^{235}\text{U}$ ,  $^{239}\text{Pu}$  and  $^{241}\text{Pu}$  between 10 keV and 2.6 MeV, in: *Proceedings of the 2nd Conference on Neutron Physics*, Kiev, 3, 1973, pp. 27–45.
- [21] I. Szabo, J.P. Marquette, Measurement of the neutron induced fission cross sections of uranium 235 and plutonium 239 in the MeV energy range, in: *Meeting on Fast Neutron Fission Cross Sections of U-233, U-238, and Pu-239*, 1976, p. 208.
- [22] P. Staples, K. Morley, Neutron-induced fission cross-section ratios for  $^{239}\text{Pu}$ ,  $^{240}\text{Pu}$ ,  $^{242}\text{Pu}$ , and  $^{244}\text{Pu}$  relative to  $^{235}\text{U}$  from 0.5 to 400 MeV, *Nucl. Sci. Eng.* 129 (2) (1998) 149–163.
- [23] P.W. Lisowski, J.L. Ullmann, S.J. Balestrini, A.D. Carlson, O.A. Wasson, N.W. Hill, Neutron induced fission cross section ratios for  $^{232}\text{Th}$ ,  $^{235,238}\text{U}$ ,  $^{237}\text{Np}$ , and  $^{239}\text{Pu}$  from 1 to 400 MeV, in: *Proceedings of the Conference on Nuclear Data for Science and Technology*, Mito 1988, Japan, 1, 1988, p. 97. EXFOR 14016004.
- [24] O. Shcherbakov, A. Donets, A. Evdokimov, A. Fomichev, T. Fukahori, A. Hasegawa, A. Laptev, V. Maslov, G. Petrov, S. Soloviev, et al., Neutron-induced fission of  $^{233}\text{U}$ ,  $^{238}\text{U}$ ,  $^{232}\text{Th}$ ,  $^{239}\text{Pu}$ ,  $^{237}\text{Np}$ ,  $^{241}\text{Pu}$  and  $^{209}\text{Bi}$  relative to  $^{235}\text{U}$  in the energy range 1–200 MeV, *J. Nucl. Sci. Technol.* 39 (sup2) (2002) 230–233.
- [25] L.W. Weston, J.H. Todd, Neutron fission cross sections of  $^{239}\text{Pu}$  and  $^{240}\text{Pu}$  relative to  $^{235}\text{U}$ , *Nucl. Sci. Eng.* 84 (3) (1983) 248–259.
- [26] L.W. Weston, J.H. Todd, Subthreshold fission cross section of  $^{240}\text{Pu}$  and the fission cross sections of  $^{235}\text{U}$  and  $^{239}\text{Pu}$ , *Nucl. Sci. Eng.* 88 (4) (1984) 567–578.
- [27] L.W. Weston, J.H. Todd, High-resolution fission cross-section measurements of  $^{235}\text{U}$  and  $^{239}\text{Pu}$ , *Nucl. Sci. Eng.* 111 (4) (1992) 415–421.
- [28] L.W. Weston, J.H. Todd, H. Derrien, Normalization and minimum values of the  $^{239}\text{Pu}$  fission cross section, *Nucl. Sci. Eng.* 115 (2) (1993) 164–172.
- [29] F. Tovesson, T.S. Hill, Cross sections for  $^{239}\text{Pu}(n,f)$  and  $^{241}\text{Pu}(n,f)$  in the range  $E_n = 0.01$  eV to 200 MeV, *Nucl. Sci. Eng.* 165 (2) (2010) 224–231.
- [30] Y. Qiu, C. Lan, Y. Chen, L. Jiang, J. Bao, Y. Yang, Z. Wen, R. Liu, X. Ruan, J. Tang, et al., Measurement of the  $^{239}\text{Pu}(n,f)$  cross section from 4 keV to 100 MeV using the white neutron source at the CSNS Back-n facility, *Phys. Rev. C* 107 (2) (2023) 024606.
- [31] R. Pérez Sánchez, B. Jurado, V. Méot, O. Roig, M. Dupuis, O. Bouldand, D. Denis-Petit, P. Marini, L. Mathieu, I. Tsekanovich, et al., Simultaneous determination of neutron-induced fission and radiative capture cross sections from decay probabilities obtained with a surrogate reaction, *Phys. Rev. Lett.* 125 (12) (2020) 122502.
- [32] L. Snyder, M. Anastasiou, N.S. Bowden, J. Bundgaard, R.J. Casperson, D.A. Cebra, T. Classen, D.H. Dongwi, N. Fotiadis, J. Gearhart, et al., Measurement of the  $^{239}\text{Pu}(n,f)/^{235}\text{U}(n,f)$  cross-section ratio with the NIFFTE fission time projection chamber, *Nucl. Data Sheet.* 178 (2021) 1–40.
- [33] D.H. Dongwi, L. Snyder, V. Aguilar, N. Androski, M. Anastasiou, N.S. Bowden, et al., Remeasurement of the  $^{239}\text{Pu}(n,f)/^{235}\text{U}(n,f)$  Cross-Section Ratio with the NIFFTE fission Time Projection Chamber Using Vapor-deposited Targets, *arXiv:2409.18279*. (2024). <https://doi.org/https://arxiv.org/abs/2409.18279v1>
- [34] G. Tagliente, et al., The n\_TOF facility at CERN, *EPJ Web Conf.* 292 (2024) 12002. <https://doi.org/10.1051/epjconf/202429212002>
- [35] E. Chiaveri, et al., The CERN n\_TOF facility: neutron beams performances for cross section measurements, *Nucl. Data Sheet.* 119 (2014) 1–4. <https://doi.org/10.1016/j.nds.2014.08.003>
- [36] C. Rubbia, et al., A high resolution spallation driven facility at the CERN PS to measure neutron cross-sections in the interval from 1-eV to 250-MeV: A Relative performance assesment, Technical Report, CERN, 1998.
- [37] R. Esposito, et al., for the n\_TOF Collaboration, Design of the third-generation lead-based neutron spallation target for the neutron time-of-flight facility at CERN, *Phys. Rev. Accel. Beam.* 24 (2021) 093001. <https://doi.org/10.1103/PhysRevAccelBeams.24.093001>
- [38] R. Esposito, M. Calviani, O. Aberle, Design, testing, commissioning, and early operation of the third-generation n\_TOF neutron spallation target at CERN, *EPJ Web Conf.* 285 (2023) 07003. <https://doi.org/10.1051/epjconf/202328507003>
- [39] C. Guerrero, et al., Performance of the neutron time-of-flight facility n\_TOF at CERN, *Eur. Phys. J. A* 49 (2013) 27. <https://doi.org/10.1140/epja/i2013-13027-6>
- [40] M. Barbagallo, et al., High-accuracy determination of the neutron flux at n\_TOF, *Eur. Phys. J. A* 49 (2013) 156. <https://doi.org/10.1140/epja/i2013-13156-x>
- [41] J. Perkowski, et al., Multi-section fission ionization chamber for measurement of  $^{239}\text{Pu}(n,\gamma)$  reaction in fission tagging method, *Nucl. Instrum. Method. Phys. Res., Sect. A* 1067 (2024) 169649. <https://doi.org/10.1016/j.nima.2024.169649>
- [42] K. Verguts, K. Van Hecke, Purification of an Am-241 contaminated Pu-239 batch, Report R-8843. SCK CEN, Belgium, 2022, (Restricted Contract Report).
- [43] G. Sibbens, A. Göök, D. Lewis, A. Moens, S. Oberstedt, D. Vanleeuw, R. Wynants, M. Zampella, Target preparation for neutron-induced reaction measurements, *EPJ Web Conf.* 229 (2020) 04003. <https://doi.org/10.1051/epjconf/202022904003>
- [44] U. Abbondanno, et al., The data acquisition system of the neutron time-of-flight facility n\_TOF at CERN, *Nucl. Instrum. Method. Phys. Res., Sect. A* 538 (1) (2005) 692–702. <https://doi.org/10.1016/j.nima.2004.09.002>
- [45] C. Guerrero, et al., The n\_TOF total absorption calorimeter for neutron capture measurements at CERN, *Nucl. Instrum. Method. Phys. Res., Sect. A* 608 (3) (2009) 424–433. <https://doi.org/10.1016/j.nima.2009.07.025>
- [46] J. Balibrea-Correa, et al., n\_TOF Collaboration, Measurement of the  $\alpha$  ratio and  $(n,\gamma)$  cross section of  $^{235}\text{U}$  from 0.2 to 200 eV at n\_TOF, *Phys. Rev. C* 102 (2020) 044615. <https://doi.org/10.1103/PhysRevC.102.044615>
- [47] C. Guerrero, E. Berthoumieux, D. Cano-Ott, E. Mendoza, S. Andriamonje, J. Andrzejewski, L. Audouin, M. Barbagallo, V. Bécares, F. Bečvář, et al., Simultaneous measurement of neutron-induced capture and fission reactions at CERN, *Eur. Phys. J. A* 48 (3) (2012) 29.
- [48] Bacak, M., et al., Preliminary results on the  $^{233}\text{U}$  capture cross section and alpha ratio measured at n\_TOF (CERN) with the fission tagging technique, *EPJ Web Conf.* 211 (2019) 03007. <https://doi.org/10.1051/epjconf/201921103007>
- [49] A. Ferrari, J. Ranft, P.R. Sala, A. Fassò, FLUKA: A multi-particle transport code (Program version 2005), CERN-2005-10, Cern, 2005.
- [50] J.A. Pavón-Rodríguez, et al., Features of the EAR2 neutron beam following the spallation target upgrade at the n\_TOF facility at CERN, 2025, <https://arxiv.org/abs/2505.00042>
- [51] J.A. Pavón-Rodríguez, et al., Characterisation of the n\_TOF 20 m beam line at CERN with the new spallation target, *EPJ Web of Conf.* 284 (2023) 06006. <https://doi.org/10.1051/epjconf/202328406006>
- [52] V. Vlachoudis, M. Sabate-Gilarte, V. Alcayne, F. Gunsing, E. Mendoza, F. Ogallar, I. Rejwan, M. Bacak, C. Guerrero, C. Massimi, A. Stamatopoulos, On the resolution function of the n\_TOF facility: a comprehensive study and user guide, Technical Report, CERN Document Server, 2021. <https://cds.cern.ch/record/2764434>.
- [53] C. Weiß, et al., The new vertical neutron beam line at the CERN n\_TOF facility design and outlook on the performance, *Nucl. Instrum. Method. Phys. Res., Sect. A* 799 (2015) 90–98. <https://doi.org/10.1016/j.nima.2015.07.027>
- [54] S. Marrone, et al., A low background neutron flux monitor for the n\_TOF facility at CERN, *Nucl. Instrum. Method. Phys. Res., Sect. A* 517 (1–3) (2004) 389–398.
- [55] I. Durán, R. Capote, P. Cabanelas, Normalization of ToF (n,f) measurements in fissile targets: microscopic cross-section integrals, *Nucl. Data Sheet.* 193 (2024) 95–104. Special Issue on Nuclear Reaction Data, <https://doi.org/10.1016/j.nds.2024.01.004>
- [56] I. Durán, R. Capote, G. Schnabel, Looking for integral references for the fission cross sections in actinides above 1 MeV, *EPJ Web Conf.* 294 (2024) 04001. <https://doi.org/10.1051/epjconf/202429404001>.
- [57] 2024, (ENDF/B-VIII.1 library available at <https://www.nndc.bnl.gov/ndf-releases/?version=B-VIII.1>). National Nuclear Data Center, Brookhaven, USA.
- [58] G. Nobre, D. Brown, R. Arcilla, R. Coles, B. Shu, Progress towards the ENDF/B-VIII.1 release, *EPJ Web of Conf.* 294 (2024) 04004. <https://doi.org/10.1051/epjconf/202429404004>
- [59] G.W. Carlson, The effect of fragment anisotropy on fission-chamber efficiency, *Nucl. Instrum. Method.* 119 (1974) 97–100. [https://doi.org/10.1016/0029-554X\(74\)90736-8](https://doi.org/10.1016/0029-554X(74)90736-8)
- [60] 2023, (INDEN evaluation for  $n+^{239}\text{Pu}$  available at [https://www.nds.iaea.org/INDEN/data/pu239e81b1\\_Pu\\_Xj\\_ENDF.zip](https://www.nds.iaea.org/INDEN/data/pu239e81b1_Pu_Xj_ENDF.zip)). International Nuclear Data Evaluation Network coordinated by the IAEA. M. Pigni, R. Capote, A. Trkov, G. Noguere, Resolved Resonance Region evaluation for  $n+^{239}\text{Pu}$  reactions.
- [61] D. Neudecker, D.L. Smith, F. Tovesson, R. Capote, M.C. White, N.S. Bowden, L. Snyder, A.D. Carlson, R.J. Casperson, V. Pronyaev, et al., Applying a template of expected uncertainties to updating  $^{239}\text{Pu}(n,f)$  cross-section covariances in the neutron data standards database, *Nucl. Data Sheet.* 163 (2020) 228–248. <https://doi.org/doi.org/10.1016/j.nds.2019.12.005>
- [62] R. Capote, G. Schnabel, A.D. Carlson, V.G. Pronyaev, G. Noguere, D. Neudecker, Experimental spectrum averaged cross sections (SACS) in  $^{252}\text{Cf}(sf)$  neutron field and its impact on the evaluation of neutron standards, *EPJ Web Conf.* 281 (2023) 00027. <https://doi.org/10.1051/epjconf/202328100027>
- [63] W. Mannhart, Status of the  $^{252}\text{Cf}(sf)$  Fission Neutron Spectrum Evaluation with Regard to Recent Experiments, Technical Report INDC(NDS)-0220, IAEA Consult. Meet. on "Physics of Neutron Emission in Fission", 1988. <https://www.nds.iaea.org/publications/indc/indc-nds-0220/>.
- [64] A. Trkov, P.J. Griffin, S.P. Simakov, L.R. Greenwood, K.I. Zolotarev, R. Capote, D.L. Aldama, V. Chechev, C. Destouches, A.C. Kahler, et al., IRDFF-II: A new neutron metrology library, *Nucl. Data Sheet.* 163 (2020) 1–108. <https://doi.org/doi.org/10.1016/j.nds.2019.12.001>
- [65] 2020, (Numerical data of the  $^{252}\text{Cf}(sf)$  reference neutron spectrum (W. Mannhart evaluation of ref. [63]) are available from the IAEA standard webpage at <https://www.nds.iaea.org/standards/ref-spectra/PFNS-Cf252sf.txt>, and also from the IRDFF-II webpage (MT 9861) at [https://nds.iaea.org/IRDFF/IRDFF-II\\_sp\\_ENDF.zip](https://nds.iaea.org/IRDFF/IRDFF-II_sp_ENDF.zip)).
- [66] O. Bersillon, L.R. Greenwood, P.J. Griffin, W. Mannhart, H.J. Nolphienus, R. Paviotti-Corcuera, K.I. Zolotarev, E.M. Zsolnay, A.L. Nichols (technical editor), International

Reactor Dosimetry File 2002 (IRDF-2002), IAEA, Vienna, Austria, TRS 452 (2006).  
[https://www-pub.iaea.org/MTCD/Publications/PDF/TRS452\\_web.pdf](https://www-pub.iaea.org/MTCD/Publications/PDF/TRS452_web.pdf).

[67] W. Mannhart, Response of activation reactions in the neutron field of  $^{252}\text{Cf}(sf)$ , 2006, (P. 30 in Ref. [66]).